

Modelling the nonlinear shear stress-strain response of glass fibre-reinforced composites. Part I: Experimental results

W. Van Paepegem*, I. De Baere and J. Degrieck

Ghent University, Dept. of Mechanical Construction and Production,
Sint-Pietersnieuwstraat 41, 9000 Gent, Belgium

Abstract

The ASTM D3518/D3518M-94(2001) Standard Test Method for "*In-Plane Shear Response of Polymer Matrix Composite Materials by Tensile Test of a $\pm 45^\circ$ Laminate*" is based on the uni-axial tensile stress-strain response of a $\pm 45^\circ$ composite laminate which is symmetrically laminated about the midplane. For long glass fibre-reinforced epoxy composites, the test shows a highly nonlinear shear stress-strain curve. This work is concerned with the development of a material model to predict this mechanical behaviour. Part I discusses the experimental program with tensile tests on $[+45^\circ/-45^\circ]_{2s}$ laminates and off-axis $[10^\circ]_8$ composites. Cyclic tensile tests have been performed to assess the amount of permanent shear strain and the residual shear modulus.

Part II focuses on the development of the material model and the finite element implementation. Two state variables have been introduced to represent the shear modulus degradation and the accumulation of permanent shear strain. The model has also been applied to the simulation of a three-point bending test on a $[+45^\circ/-45^\circ]_{2s}$ laminate.

Keywords A: Polymer-matrix composites (PMCs); B: Mechanical properties; C: Damage mechanics; D: Mechanical testing.

1. Introduction

Several test methods have been proposed to determine the inplane shear stress-strain response of a fibre-reinforced composite [2]. The ASTM D4255/D4255M-01 Standard Test Method for "*In-Plane Shear Properties of Polymer Matrix Composite Materials by the Rail Shear Method*" uses the three- or two-rail shear test. The ASTM D5379/D5379M-98 Standard Test Method for "*Shear Properties of Composite Materials by the V-Notched Beam Method*" is another example.

As these standards require specialized fixtures, the inplane shear stress-strain response is often determined by using the ASTM D3518/D3518M-94(2001) Standard Test Method for "*In-Plane Shear Response of Polymer Matrix Composite Materials by Tensile Test of a $\pm 45^\circ$ Laminate*" (or the equivalent ISO 14129:1997 Standard "*Fibre-reinforced plastic composites - Determination of the in-plane shear stress/shear strain response, including the in-plane shear modulus and strength, by the plus or minus 45 degree tension test method*"). This standard is based on the uni-axial stress-strain response of a $\pm 45^\circ$ laminate which is symmetrically laminated about the midplane.

* Corresponding author (Fax: +32-(0)9-264.35.87, E-mail: Wim.VanPaepegem@UGent.be).

In this work, the latter standard is used to study the nonlinear shear stress-strain response of a long glass fibre-reinforced epoxy composite. Also, a comparison is made with the 10° off-axis tensile test, which has received much attention during the last decade [3-8].

Part I discusses the experimental results for the static tensile tests on [+45°/-45°]_{2s} laminates and off-axis [10°]₈ composites. Also, cyclic tensile tests on [+45°/-45°]_{2s} laminates have been performed.

In Part II [1], the development of the material model is treated. Two state variables are introduced to describe the nonlinear shear stress-strain response of the long glass fibre-reinforced epoxy composite. All results are validated with finite elements.

2. Material and experimental set-up

2.1. Material

The material under study was a glass/epoxy composite. The glass reinforcement was a unidirectional E-glass fabric (Roviglas R17/475). In the fibre direction \bar{e}_{11} , the reinforcement was 475 g/m², while in the direction \bar{e}_{22} , the reinforcement was 17 g/m². The epoxy matrix was Araldite LY 556.

Four stacking sequences were manufactured: [0°]₈, [90°]₈, [+45°/-45°]_{2s} and [10°]₈, with the angle referred to the direction \bar{e}_{11} . The layups [0°]₈ and [90°]₈ were used for characterization in the orthotropic material directions, while [+45°/-45°]_{2s} and [10°]₈ were used for shear tests. All specimens were manufactured by vacuum assisted resin transfer moulding with a closed steel mould. The thickness of all specimens was 3.0 mm and the fibre volume fraction was about 50 %. The samples were cut to dimensions on a water-cooled diamond saw.

The inplane elastic properties of the individual glass/epoxy lamina were determined by the dynamic modulus identification method described by Sol et al. [9,10] and are listed in Table 1.

Table 1 Inplane elastic properties of the individual glass/epoxy lamina (dynamic modulus identification method).

E_{11} [GPa]	38.9
E_{22} [GPa]	13.3
ν_{12} [-]	0.258
G_{12} [GPa]	5.13

Apart from the dynamic modulus identification method, static tensile tests on the [0°]₈ and [90°]₈ layups have been performed to check the values of the elastic properties and to determine the static strengths. It is important to mention that the mechanical behaviour in the \bar{e}_{11} and \bar{e}_{22} direction is linear up till failure. This is demonstrated for the \bar{e}_{22} direction in Figure 1.

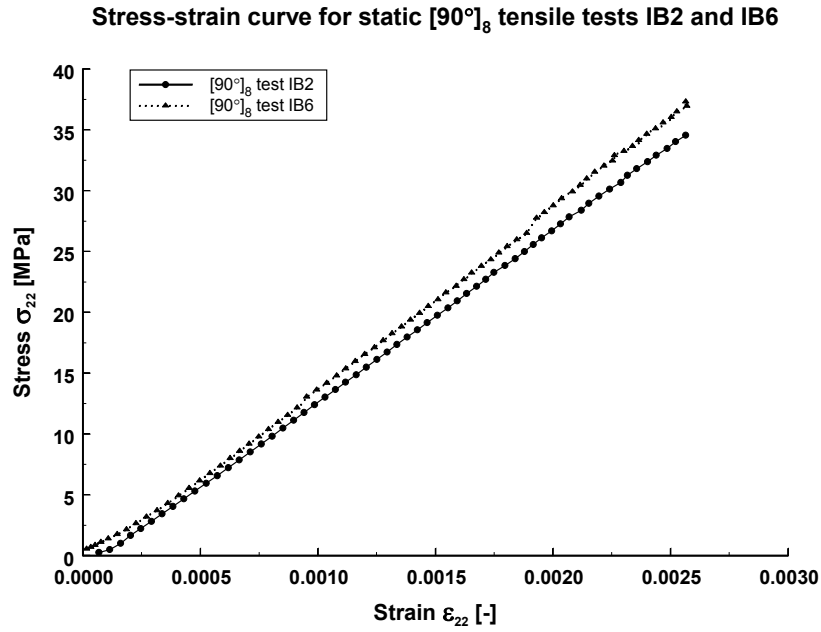


Figure 1 Stress-strain curve for static $[90^\circ]_8$ tensile tests IB2 and IB6.

The elastic properties, calculated from the mechanical tests, are listed in Table 2. If compared to the values in Table 1, the agreement is satisfactory.

Table 2 Inplane elastic properties of the individual glass/epoxy lamina (mechanical testing).

E_{11} [GPa]	42.4
E_{22} [GPa]	14.2
ν_{12} [-]	0.245

The tensile strength properties were determined from the $[0^\circ]_8$ and $[90^\circ]_8$ stacking sequence and are listed in Table 3.

Table 3 Tensile strength properties of the individual glass/epoxy lamina.

X_T [MPa]	901.0 ± 38.0
ϵ_{11}^{ult} [-]	0.025
Y_T [MPa]	36.5 ± 1.1
ϵ_{22}^{ult} [-]	0.0025

2.2. Experimental set-up

For characterization of the shear behaviour of the glass/epoxy composite, tensile tests were performed on the $[+45^\circ/-45^\circ]_{2s}$ and $[10^\circ]_8$ stacking sequence.

All tensile tests were performed on an electromechanical Instron testing machine with a loadcell of ± 100 kN. The tests were displacement-controlled with a speed of 2 mm/min and both load and displacement were recorded.

The layout of the specimens is illustrated in Figure 2.

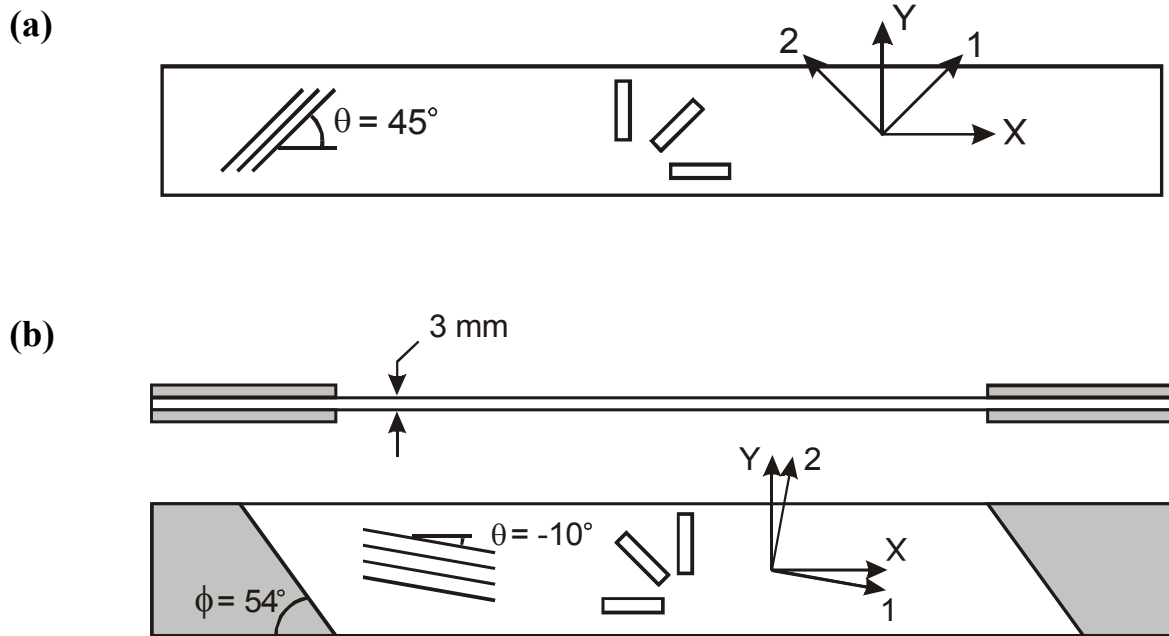


Figure 2 Layout of the (a) $[+45^\circ/-45^\circ]_{2s}$ specimens and (b) $[10^\circ]_8$ specimens.

All specimens were instrumented with three separate strain gauges, in the 0° , 45° and 90° direction respectively. A strain gauge rosette was not suitable, because the difference in magnitude between the three strains ε_{xx} , $\varepsilon_{\alpha\alpha}$ ($\alpha = 45^\circ$) and ε_{yy} was too large. As a consequence the strain gauge rosette was distorted and came loose very quickly. For example, for a typical $[+45^\circ/-45^\circ]_{2s}$ tensile test, the measured values for ε_{xx} and ε_{yy} just before saturation of the strain gauges were 3.62 % and -3.67 %.

In case of the $[+45^\circ/-45^\circ]_{2s}$ specimens, the measured value of the strain $\varepsilon_{\alpha\alpha}$ ($\alpha = 45^\circ$) was only used as a check, since the strains ε_{11} and ε_{22} can be calculated from ε_{xx} and ε_{yy} only, because γ_{xy} should be zero. It appeared that this hypothesis was valid, because the maximum value of γ_{xy} observed was 0.09 %, just before saturation of the strain gauges of $[+45^\circ/-45^\circ]_{2s}$ specimen IH4. In all other specimens, the maximum value was even lower.

Concerning the $[10^\circ]_8$ specimens, the choice of the tabs is of particular importance. Already in 1968, Pagano and Halpin pointed out that the end constraints induce shear forces and bending moments in off-axis composite specimens. During the last few years, several papers have been published about the use of oblique end tabs in case of off-axis specimens [4-7]. It has been shown by Pierron et al. that the use of oblique tabs significantly increases the maximum shear stress at failure and results in a homogeneous strain field over the whole specimen [5,7]. Sun and Chung [4] calculated that the optimal oblique angle ϕ corresponds with the angle between the X-axis and the theoretical line of iso-displacements. The angle ϕ is calculated as:

$$\cot \phi = \frac{-\bar{S}_{16}}{\bar{S}_{11}} \quad (1)$$

where \bar{S}_{11} and \bar{S}_{16} are the components of the stiffness tensor in the axes (X,Y). For the glass/epoxy material under study, the angle ϕ is 54° .

The tabs are made of the same glass/epoxy material with the stacking sequence $[+45^\circ/-45^\circ]_{2s}$.

3. Static tensile tests on the $[+45^\circ/-45^\circ]_{2s}$ and $[10^\circ]_8$ stacking sequence

3.1. $[+45^\circ/-45^\circ]_{2s}$ specimens

For the $[+45^\circ/-45^\circ]_{2s}$ specimens, the ASTM D3518/D3518M-94(2001) Standard Test Method for "In-Plane Shear Response of Polymer Matrix Composite Materials by Tensile Test of a $\pm 45^\circ$ Laminate" is applied. The shear stress τ_{12} and the shear strain γ_{12} are calculated as follows:

$$\begin{aligned} \tau_{12}^i &= \frac{F^i}{2 \cdot b \cdot d} \\ \gamma_{12}^i &= \varepsilon_{xx}^i - \varepsilon_{yy}^i \end{aligned} \quad (2)$$

where:

- F^i [N] = load at the i^{th} point of $[+45^\circ/-45^\circ]_{2s}$ load-deformation curve
- τ_{12}^i [MPa] = shear stress at the i^{th} point of the shear stress-strain curve
- γ_{12}^i [-] = shear strain at the i^{th} point of the shear stress-strain curve
- ε_{xx}^i [-] = longitudinal strain at the i^{th} point of $[+45^\circ/-45^\circ]_{2s}$ load-deformation curve
- ε_{yy}^i [-] = transverse strain at the i^{th} point of $[+45^\circ/-45^\circ]_{2s}$ load-deformation curve
- b [mm] = specimen width
- d [mm] = specimen thickness

Figure 3 shows the shear stress-strain curve for the static $[+45^\circ/-45^\circ]_{2s}$ tensile tests IH4 and IG2. The calculated stiffnesses G_{12}^0 for IH4 and IG2 are 5.09 GPa and 4.66 GPa, respectively. They correspond quite well with the dynamic modulus identification measurements (see Table 1). At a shear strain γ_{12} of about 7 %, the strain gauges in the X- and Y-direction are saturating. However, the specimen only fails at a shear stress of 69.2 MPa for IH4 and 71.0 MPa for IG2. As can be seen, the results are very reproducible. Two more experiments have been done and do show the same shear stress-strain response.

Shear stress-strain curve for static $[+45^\circ/-45^\circ]_{2s}$ tests IH4 and IG2

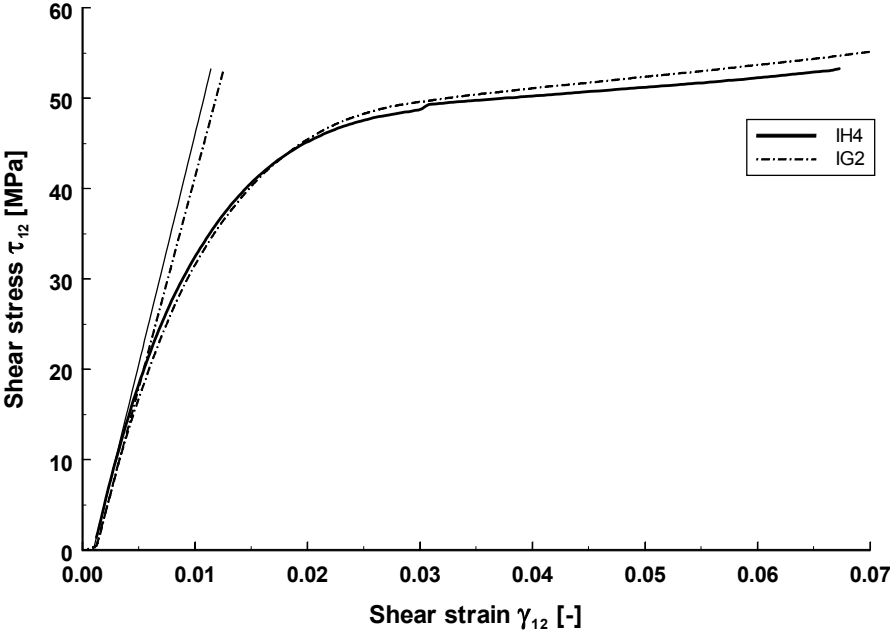


Figure 3 Shear stress-strain curve for the static $[+45^\circ/-45^\circ]_{2s}$ tensile tests IH4 and IG2.

Figure 4 shows the typical failure pattern of two tested $[+45^\circ/-45^\circ]_{2s}$ glass/epoxy laminates. As can be seen, the damage is very equally distributed along the specimen length and failure occurs in the midsection, away from the clamps. It is clearly a shear-dominated failure.

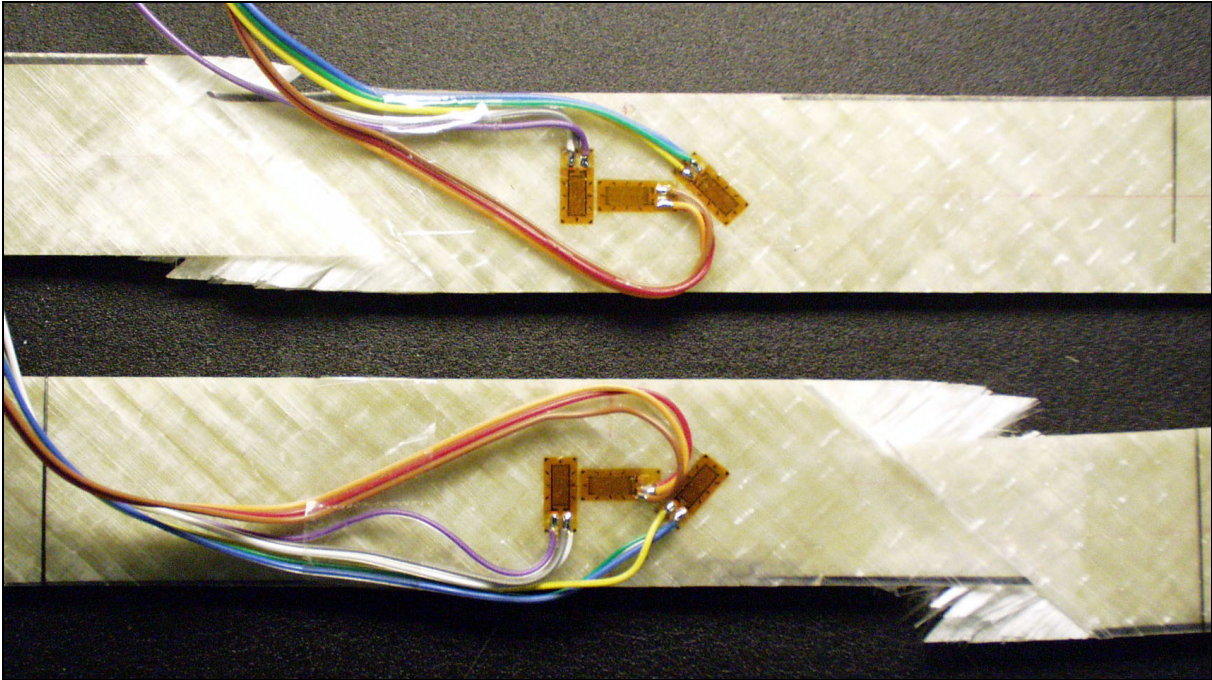


Figure 4 Typical failure patterns from static $[+45^\circ/-45^\circ]_{2s}$ tensile tests.

Figure 5 shows the time history of the measured strains for IH4 after rotation to the orthotropic material directions \bar{e}_{11} and \bar{e}_{22} . As $\gamma_{xy} = 0$, it can be easily calculated that:

$$\varepsilon_{11} = \varepsilon_{22} = \frac{\varepsilon_{xx} + \varepsilon_{yy}}{2} \quad (3)$$

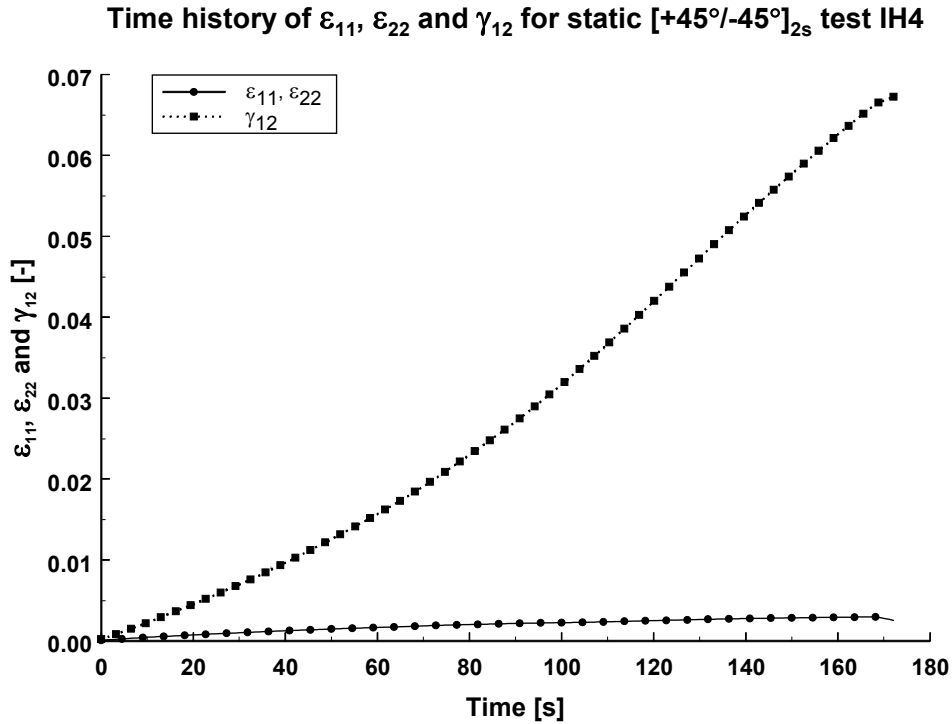


Figure 5 Time history of the measured strains ε_{11} , ε_{22} and γ_{12} for the static $[+45^\circ/-45^\circ]_{2s}$ tensile test IH4.

Figure 6 shows the time history of the measured strains for the test IG2. The time scale of Figure 6 is slightly different, because all experiments were performed with the same displacement speed (2 mm/min), but the specimen length of IH4 and IG2 was different.

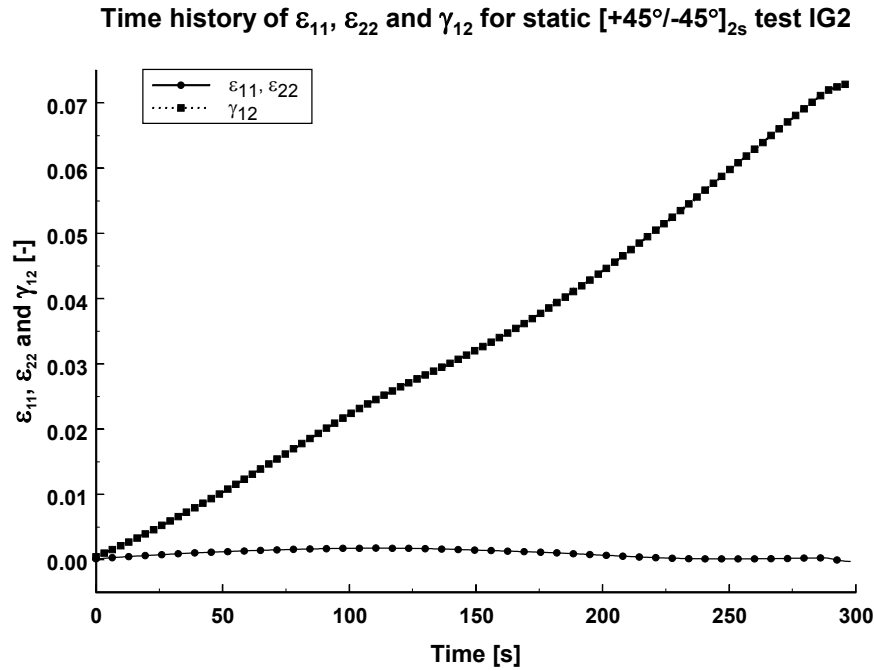


Figure 6 Time history of the measured strains ϵ_{11} , ϵ_{22} and γ_{12} for the static $[+45^\circ/-45^\circ]_{2s}$ tensile test IG2.

Summarized the static tensile tests on the $[+45^\circ/-45^\circ]_{2s}$ specimens show a pronounced nonlinear shear behaviour. At a shear strain γ_{12} of about 7 %, the strain gauges are saturating. The strains ϵ_{11} and ϵ_{22} remain very small and the assumption that γ_{xy} is zero, appears valid.

3.2. $[10^\circ]_8$ specimens

To assess the relevance of the $[10^\circ]_8$ off-axis test for shear characterization, tensile tests on the $[10^\circ]_8$ stacking sequence have been performed. Again, three strain gauges have been applied, as was already demonstrated in Figure 2.

Figure 7 shows the shear stress-strain curve for the static $[10^\circ]_8$ tensile tests IC3 and IC4. Here, the strain gauges were active up till failure. The failure shear stresses for IC3 and IC4 were 48 MPa and 53.8 MPa respectively. The failure shear strains γ_{12} were 1.7 % and 2.2 %. Both the failure shear stress and failure shear strain are considerably lower than for the $[+45^\circ/-45^\circ]_{2s}$ tensile tests. The measured shear modulus G_{12}^0 equals 5.82 GPa for IC3, but only 4.67 GPa for IC4.

Shear stress-strain curve for static $[10^\circ]_8$ tests IC3 and IC4

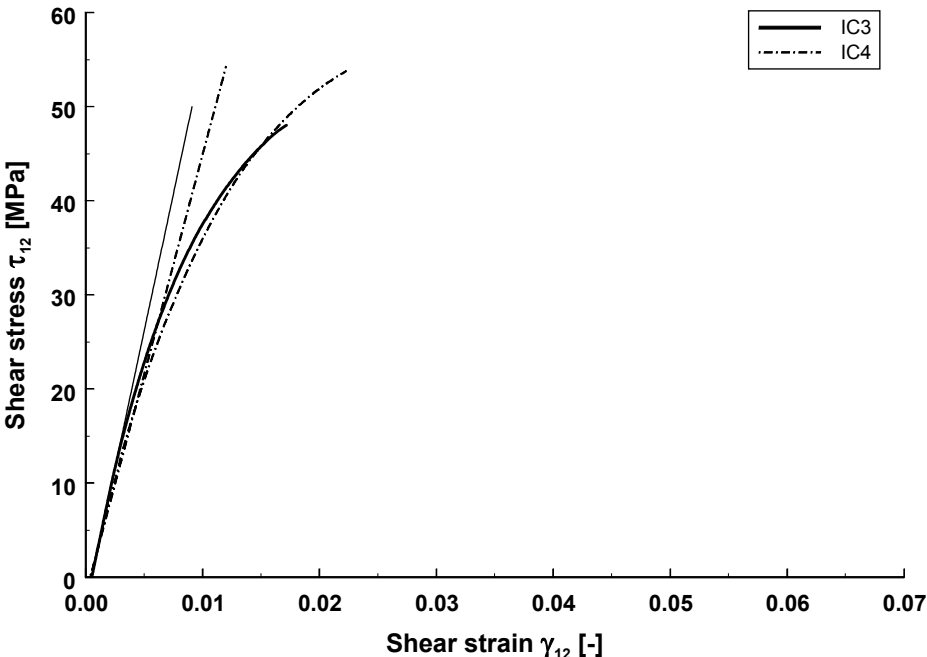


Figure 7 Shear stress-strain curve for the static $[10^\circ]_8$ tensile tests IC3 and IC4.

Figure 8 shows the typical failure patterns of two tested $[10^\circ]_8$ glass/epoxy laminates. The specimens shears off along the 10° fibre direction and very little damage can be observed in the rest of the specimen. The picture also shows the oblique end tabs with the optimal angle ϕ of 54° .

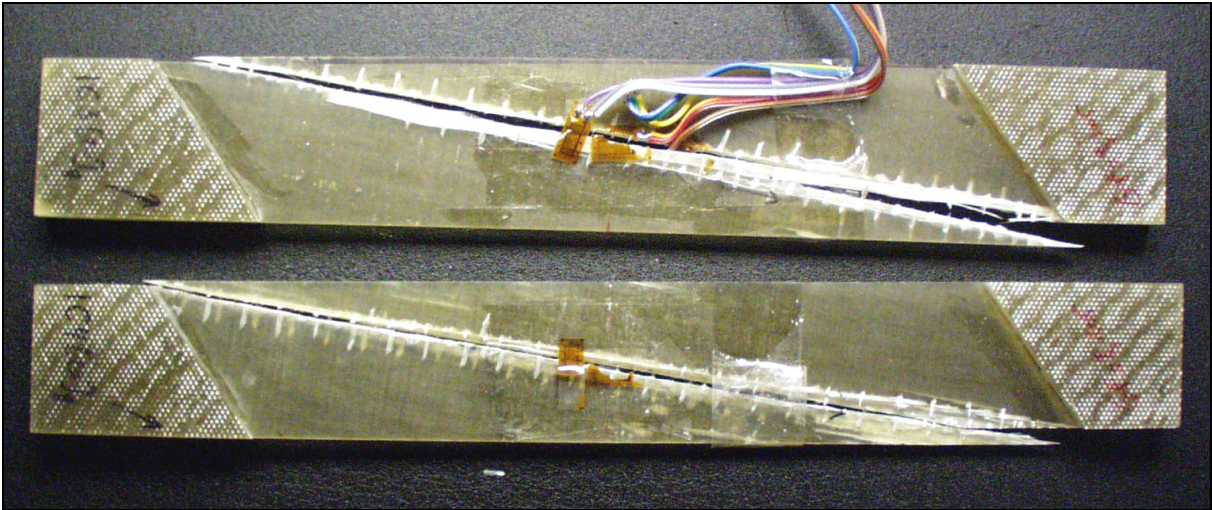


Figure 8 Typical failure patterns from static $[10^\circ]_8$ tensile tests.

Figure 9 shows the time history of the measured strains for IC3 after rotation to the orthotropic material directions \bar{e}_{11} and \bar{e}_{22} . It is important to observe that the strain ϵ_{22} is compressive, while the resulting stress σ_{22} is tensile. Using Classical Laminated Plate Theory and the elastic properties in Table 1, the strain state $(\epsilon_{11}, \epsilon_{22}, \gamma_{12}) = (0.0065, -0.0010, 0.0171)$ just before failure would result in a corresponding stress state $(\sigma_{11}, \sigma_{22}, \tau_{12}) = (254.6 \text{ MPa}, 8.98 \text{ MPa}, 87.66 \text{ MPa})$. Of course, this linear elastic calculation is only an approximation.

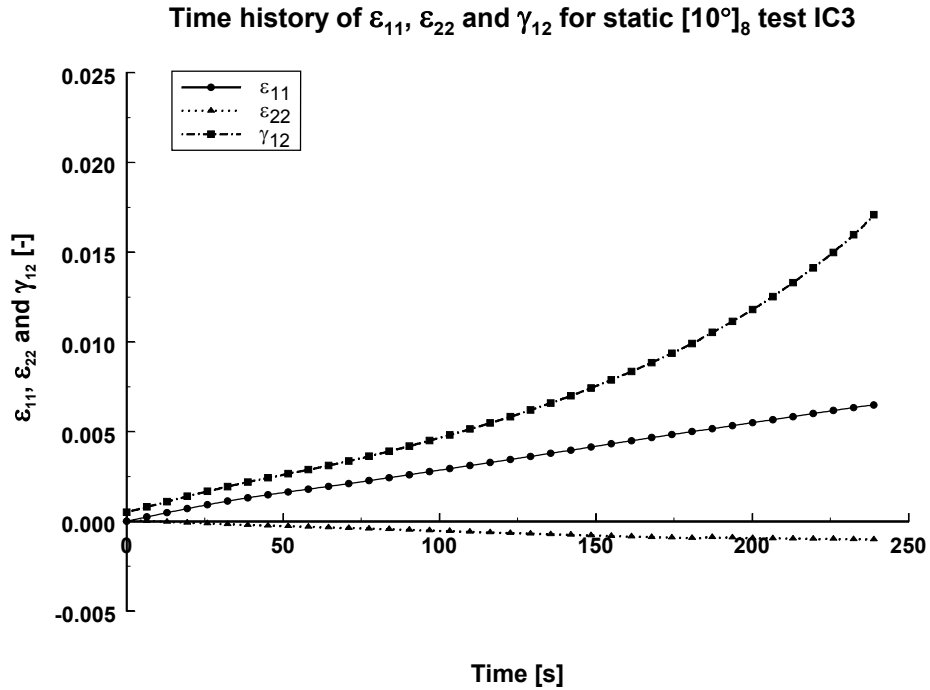


Figure 9 Time history of the measured strains ϵ_{11} , ϵ_{22} and γ_{12} for the static $[10^\circ]_8$ tensile test IC3.

Figure 10 shows the time history of the measured strains in the orthotropic material directions \bar{e}_{11} and \bar{e}_{22} for IC4.

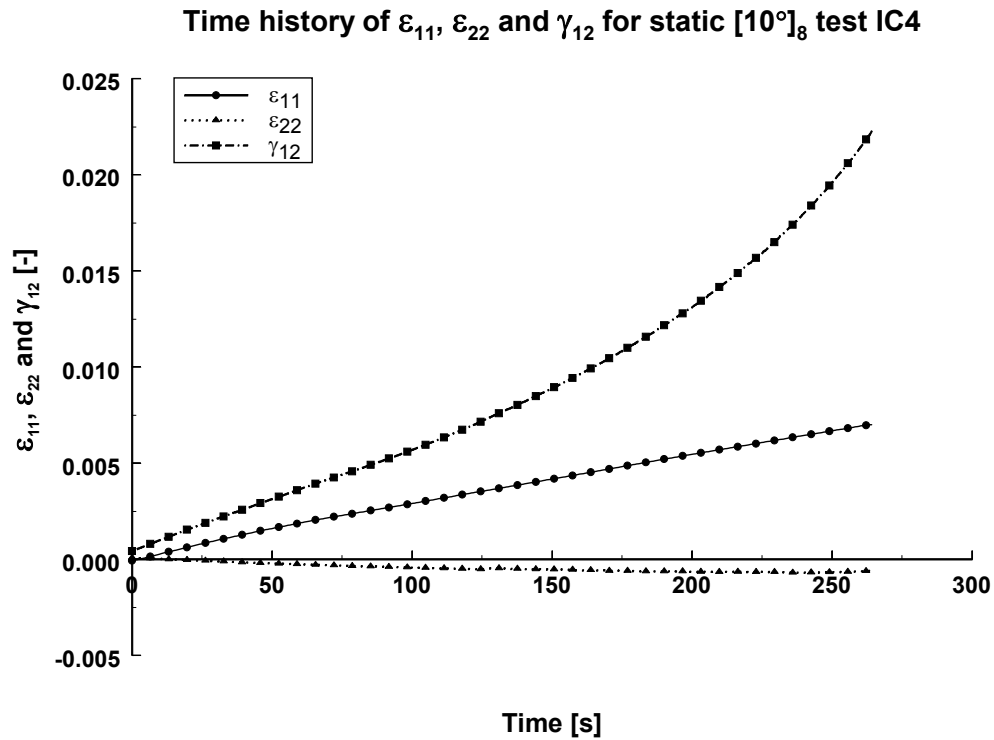


Figure 10 Time history of the measured strains ϵ_{11} , ϵ_{22} and γ_{12} for the static $[10^\circ]_8$ tensile test IC4.

It is clear that the shear stress-strain curve shows a strongly nonlinear behaviour, especially for the $[+45^\circ/-45^\circ]_{2s}$ composite specimens. In order to investigate the contribution of stiffness degradation and permanent shear strain to this phenomenon, cyclic tensile tests on the $[+45^\circ/-45^\circ]_{2s}$ specimens have been performed. These tests are discussed in the next paragraph.

4. Cyclic tensile tests on the $[+45^\circ/-45^\circ]_{2s}$ stacking sequence

In case of the cyclic tensile tests, five to ten consecutive loading-unloading cycles have been applied to the $[+45^\circ/-45^\circ]_{2s}$ stacking sequence. The displacement speed of 2 mm/min was the same as for the static tensile tests.

Figure 11 shows the load-displacement curve for the first cyclic $[+45^\circ/-45^\circ]_{2s}$ tensile test IH6. In this tests, the unloading has been done until the level of 1 kN was reached in order to maintain the grip pressure.

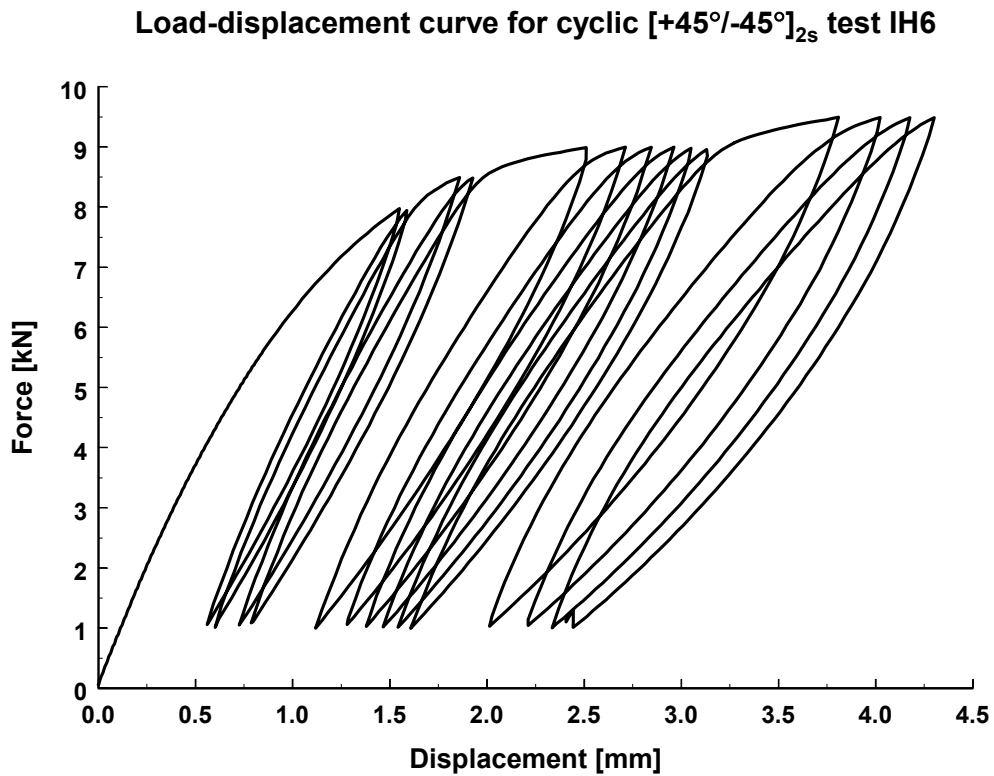


Figure 11 Load-displacement curve for the cyclic $[+45^\circ/-45^\circ]_{2s}$ tensile test IH6.

The corresponding shear stress-strain curve is shown in Figure 12. It is clear from this Figure that a considerable permanent shear strain is built up during the consecutive cycles.

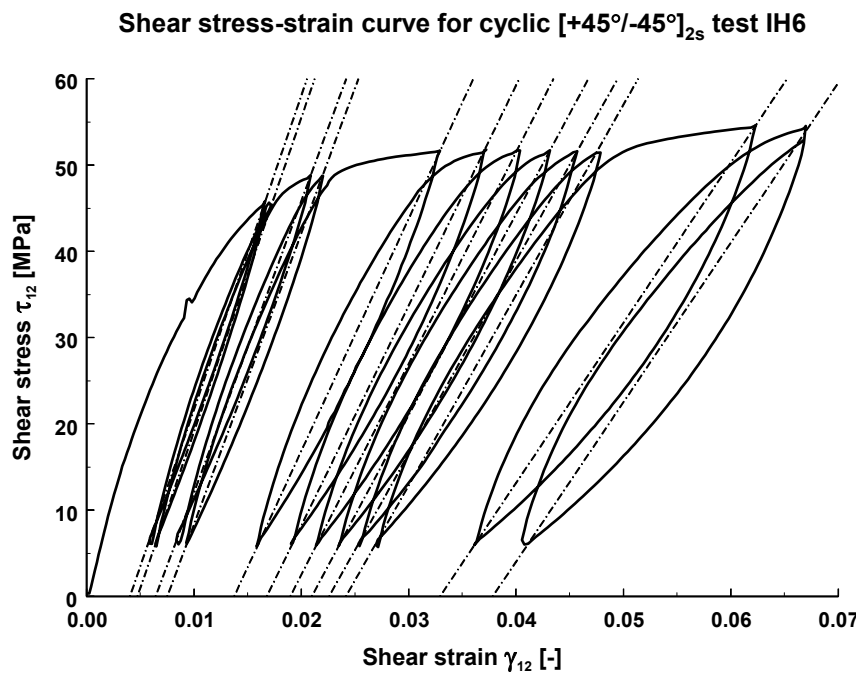


Figure 12 Shear stress-strain curve for the cyclic $[+45^\circ/-45^\circ]_{2s}$ tensile test IH6.

Figure 13 shows the corresponding time history of the measured strains in the orthotropic material directions $\bar{\epsilon}_{11}$ and $\bar{\epsilon}_{22}$.

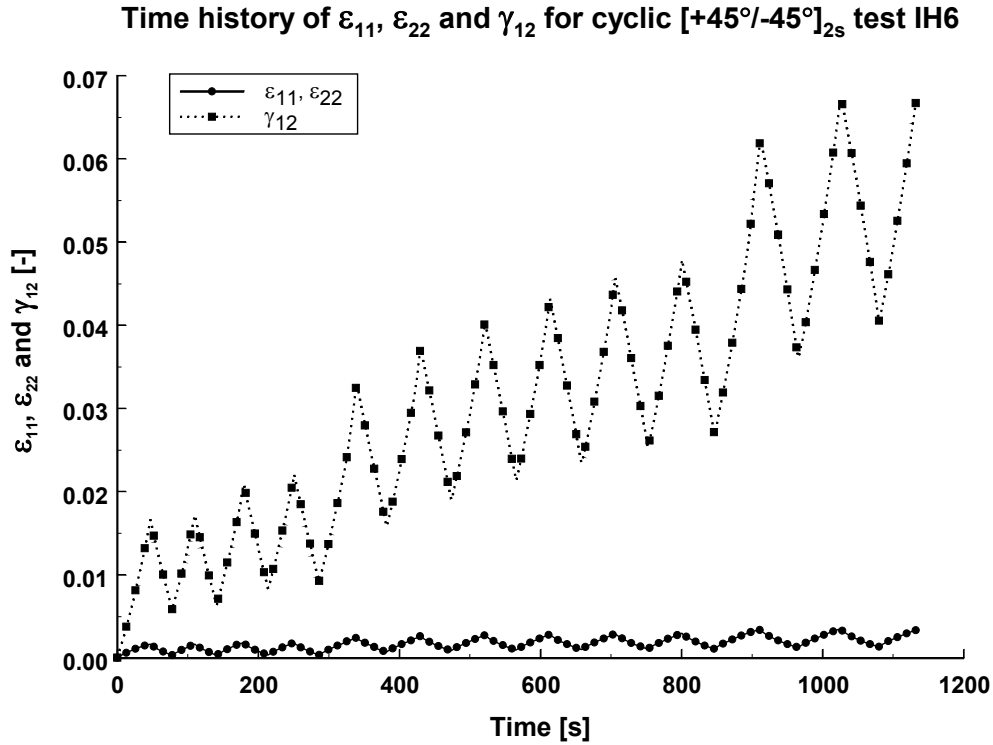


Figure 13 Time history of the measured strains ϵ_{11} , ϵ_{22} and γ_{12} for the cyclic $[+45^\circ/-45^\circ]_{2s}$ tensile test IH6.

To characterize the degradation of the shear properties, two variables are introduced: (i) the shear damage D_{12} and (ii) the permanent shear strain γ_{12}^p . They are defined by the following constitutive relations:

$$\begin{aligned} \tau_{12} &= G_{12}^0 \cdot (1 - D_{12}) \cdot (\gamma_{12} - \gamma_{12}^p) \\ D_{12} &= 1 - \frac{G_{12}^*}{G_{12}^0} \end{aligned} \quad (4)$$

where G_{12}^0 is the virgin shear modulus and G_{12}^* is the shear modulus of the damaged material. The shear modulus G_{12}^* is defined as the secant shear modulus for one loading-unloading cycle, as is illustrated in Figure 14. This definition is in agreement with the definition used by Lafarie-Frenot and Touchard in their study about the inplane shear behaviour of long carbon-fibre composites [11].

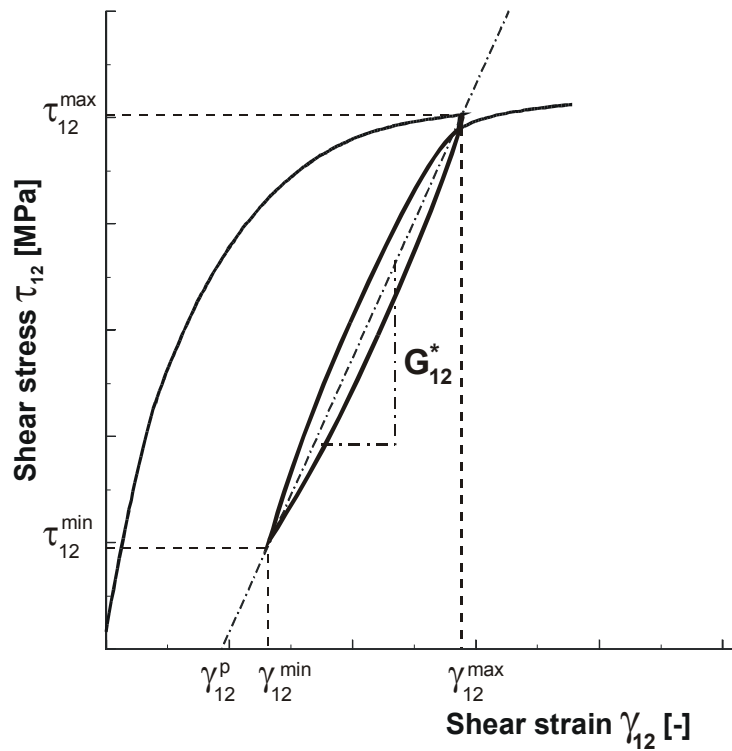


Figure 14 Definition of the shear modulus G_{12}^* and the permanent shear strain γ_{12}^p .

In the second cyclic test, shown in Figure 15, it is investigated if any apparatus effects could affect the hysteresis loops. Therefore, after unloading until 0 kN, the test is stopped for a few seconds, the grip pressure is checked and the reloading is started. As such, each reloading curve is uncoupled from the previous unloading curve. As is clearly illustrated, the hysteresis loops do show the same behaviour. In the same graph the shear stress-strain curve from the static $[+45^\circ/-45^\circ]_{2s}$ tensile test IH4 is plotted as well. The subsequent maxima of the shear stress from the cyclic test seem to follow the static envelope very well. Also the failure shear stress is quite similar: 72.5 MPa for IH2 compared to 69.2 MPa for IH4.

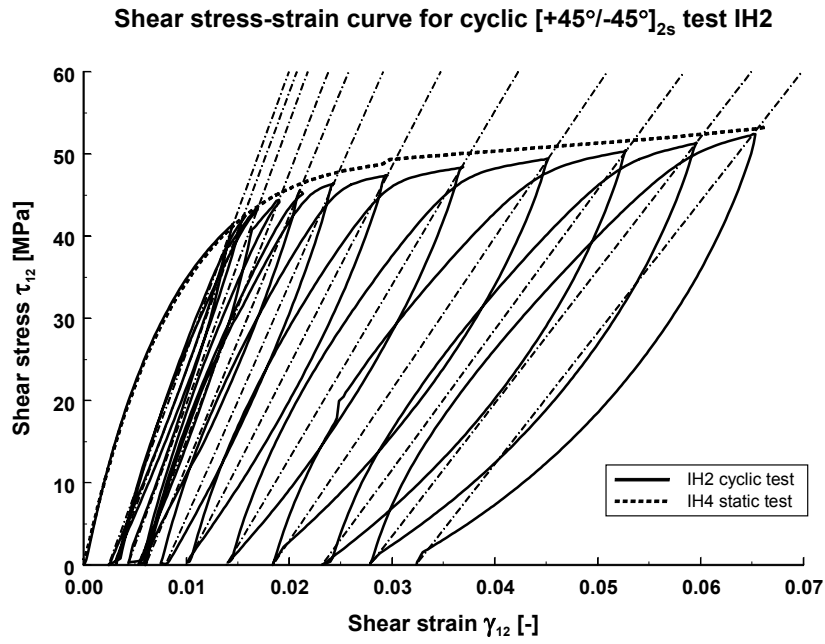


Figure 15 Shear stress-strain curve for the cyclic $[+45^\circ/-45^\circ]_{2s}$ tensile test IH2.

Figure 16 shows the corresponding time history of the measured strains in the orthotropic material directions \bar{e}_{11} and \bar{e}_{22} .

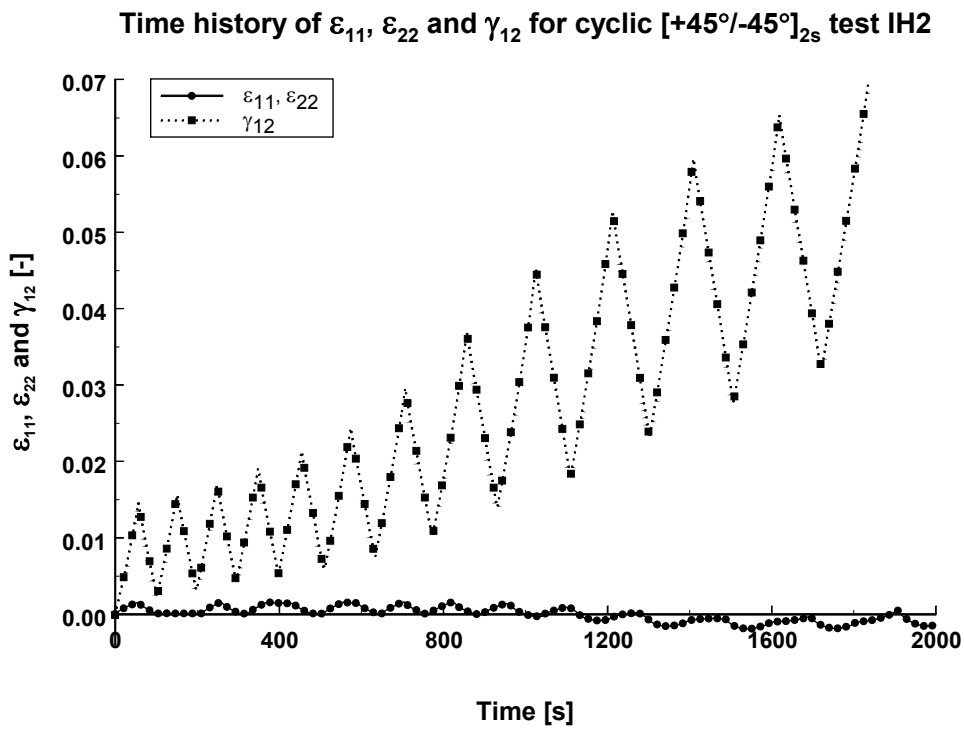


Figure 16 Time history of the measured strains ε_{11} , ε_{22} and γ_{12} for the cyclic $[+45^\circ/-45^\circ]_{2s}$ tensile test IH2.

Finally, Figure 17 shows the recorded shear stress-strain curve for the cyclic $[+45^\circ/-45^\circ]_{2s}$ tensile test IG4. The failure shear stress was 67.0 MPa in this case.

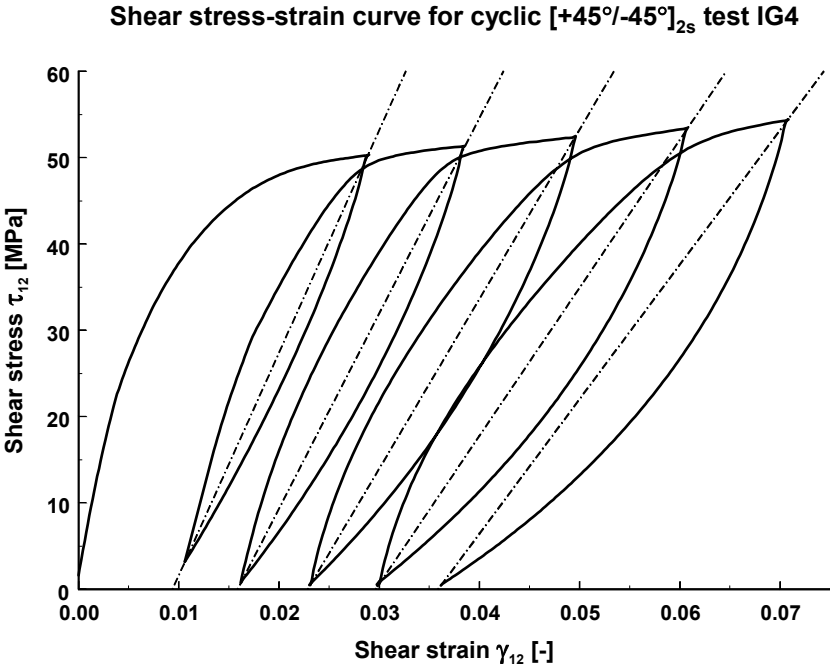


Figure 17 Shear stress-strain curve for the cyclic $[+45^\circ/-45^\circ]_{2s}$ tensile test IG4.

Figure 18 shows the time history of the measured strains in the orthotropic material directions \vec{e}_{11} and \vec{e}_{22} .

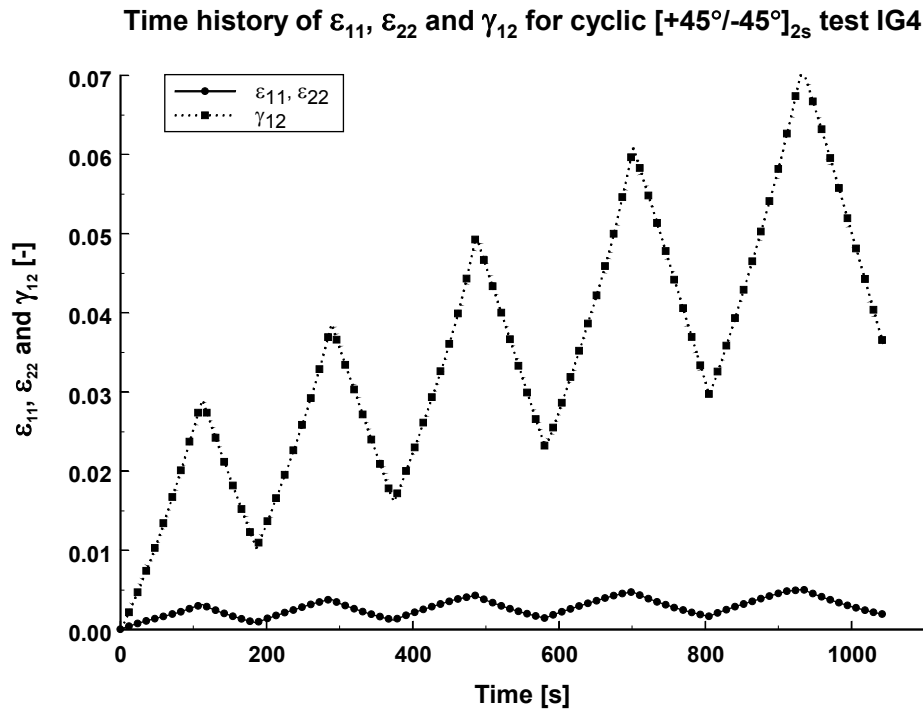


Figure 18 Time history of the measured strains ε_{11} , ε_{22} and γ_{12} for the cyclic $[+45^\circ/-45^\circ]_{2s}$ tensile test IG4.

4. Conclusions

Uni-axial tensile tests on $[+45^\circ/-45^\circ]_{2s}$ glass/epoxy composites have shown that the shear stress-strain response is highly nonlinear, with large shear strains before failure. Similar tensile tests on off-axis $[10^\circ]_8$ composites resulted in a lower shear strength and failure shear strain, but an apparently higher shear modulus.

Cyclic tensile tests on the $[+45^\circ/-45^\circ]_{2s}$ stacking sequence were performed to study the shear modulus degradation and the accumulation of permanent shear strain.

It can be concluded that the secant shear modulus of the glass/epoxy composite is decreasing considerably before failure, but also the amount of permanent shear strain is very large. The tensile tests show reproducible results and the strains ε_{11} and ε_{22} stay sufficiently small.

In part II, the observed mechanical shear behaviour will be modelled.

Acknowledgements

The author W. Van Paepegem gratefully acknowledges his finance through a grant of the Fund for Scientific Research – Flanders (F.W.O.).

References

- [1] Van Paepegem, W., De Baere, I. and Degrieck, J. (2005). Modelling the nonlinear shear stress-strain response of glass fibre-reinforced composites. Part II: Model development and finite element simulations. *Composites Science and Technology*, this issue.
- [2] Tarnopol'skii, Y.M., Arnautov, A.K. and Kulakov, V.L. (1999). Methods of determination of shear properties of textile composites. *Composites Part A: Applied Science and Manufacturing*, 30, 879-885.

- [3] Cain, K.J., Glinka, G. and Plumtree, A. (2003). Damage evolution in an off-axis unidirectional graphite bismaleimide composite loaded in tension. *Composites Part A: Applied Science and Engineering*, 34, 987-993.
- [4] Sun, C.T. and Chung, I. (1993). An oblique end-tab design for testing off-axis composite specimens. *Composites*, 24(8), 619-623.
- [5] Pierron, F. and Vautrin, A. (1996). The 10deg off-axis tensile test: a critical approach. *Composites Science and Technology*, 56, 483-488.
- [6] Pierron, F. and Vautrin, A. (1997). New ideas on the measurement of the in-plane shear strength of unidirectional composites. *Journal of Composite Materials*, 31(9), 889-895.
- [7] Pierron, F., Alloba, E., Surrel, Y. and Vautrin, A. (1998). Whole-field assessment of the effects of boundary conditions on the strain field in off-axis tensile testing of unidirectional composites. *Composites Science and Technology*, 58, 1939-1947.
- [8] Odegard, G. and Kumosa, M. (2000). Determination of shear strength of unidirectional composite materials with the Iosipescu and 10 degree off-axis shear tests. *Composites Science and Technology*, 60, 2917-2943.
- [9] Sol, H. and de Wilde, W.P. (1988). Identification of elastic properties of composite materials using resonant frequencies. In : Brebbia, C.A., de Wilde, W.P. and Blain, W.R. (eds.). *Proceedings of the International Conference "Computer Aided Design in Composite Material Technology"*, Southampton, 1988, Springer-Verlag, pp. 273-280.
- [10] Sol, H. (1990). Identification of the complex moduli of composite materials by a mixed numerical/experimental method. In : de Wilde, W.P. and Blain, W.R. (eds.). *Proceedings of the second International Conference on Computer Aided Design in Composite Material Technology*, Brussels, 25-27 April 1990, Springer-Verlag, pp. 267-279.
- [11] Lafarie-Frenot, M.C. and Touchard, F. (1994). Comparative in-plane shear behaviour of long-carbon-fibre composites with thermoset or thermoplastic matrix. *Composites Science and Technology*, 52, 417-425.